

Minimum sustainable drag for constant volume-flux pipe flows

Ivan Marusic, D. D. Joseph, and Krishnan Mahesh

Department of Aerospace Engineering and Mechanics
University of Minnesota, Minneapolis, MN 55455, USA

Abstract. Comparisons are made between laminar and turbulent flows in pipes with and without flow control, and a formula is derived that shows just how much the discrepancy between the volume flux of laminar and turbulent flow at the same pressure gradient increases as the pressure gradient is increased. Related to this, we investigate the lowest bound for skin-friction drag in pipes for flow control schemes that use surface blowing and suction with zero-net volume-flux addition.

Key words: Drag reduction, Pipe flow, Wall turbulence

1 Introduction

Recently, an analysis was presented in ref. [1] (hereafter referred to as MJM) that considered laminar and turbulent comparisons in channel flow, with and without flow control. The study focused on the control strategies that use zero-net volume-flux blowing/suction at the no-slip walls, and presented a criterion for achieving sub-laminar drag conditions. The criterion was used to gain insight into why the control strategy of Min *et al.* [2] was successful in achieving sub-laminar conditions, and how other improved strategies could perhaps be designed.

Here we extend the analysis by MJM to pipe flows, and consider implications at high Reynolds number.

2 Equations for pipe flow

For fully developed pipe flow of an incompressible fluid, driven by a constant pressure gradient, the Navier-Stokes and continuity equations may be written as

$$\frac{\partial \mathbf{V}}{\partial t} + \mathbf{V} \cdot \nabla \mathbf{V} = -\nabla p + \mathbf{e}_x P + \nabla^2 \mathbf{V}, \quad (1)$$

$$\nabla \cdot \mathbf{V} = 0. \quad (2)$$

Here we use cylindrical polar co-ordinates (r, θ, x) , where the x axis is at the pipe center and r is the radial distance from the center of the pipe. Unless indicated, all terms have been nondimensionalized using ν , the kinematic viscosity of the fluid, and a , the radius of the pipe. The domain occupied by the fluid is

$$-\infty < x < \infty; 0 \leq \theta < 2\pi; 0 \leq r \leq 1.$$

Here $P > 0$ is the constant pressure gradient driving the flow, and the total pressure at a point in the fluid is $p(r, \theta, x, t) - Px$, where in all cases pressure has been normalized by ρ , the fluid density. We denote a cylinder average with an overbar:

$$\bar{f}(r, t) = \lim_{L \rightarrow \infty} \frac{1}{2L} \int_{-L}^L \frac{1}{2\pi} \int_0^{2\pi} f(r, \theta, x, t) d\theta dx,$$

and the over-all average as

$$\langle f \rangle = 2 \int_0^1 \bar{f} r dr.$$

Therefore, the Reynolds number $Re_B = \langle \bar{V}_x \rangle$ is that based on the pipe radius and the bulk velocity. We will also decompose the velocity and pressure into mean (cylinder averaged) and fluctuating parts

$$[V_x, V_\theta, V_r, p] = [\bar{V}_x + u, \bar{V}_\theta + v, \bar{V}_r + w, \bar{p} + p'] \quad (3)$$

where the fluctuations have a zero mean: $\bar{u}, \bar{v}, \bar{w}, \bar{p}' = 0$.

The boundary conditions for pipe flow with zero-net-volume flux blowing-suction flow control are

$$V_x = V_\theta = 0; V_r = \phi(x, \theta, t) \text{ at } r = 1,$$

Note that $u = v = 0$, and $w = \phi$ at $r = 1$.

2.1 Energy equations

In the following we will make use of energy identities. These are derived first by substituting (3) into (1) and using continuity to give

$$\frac{\partial \bar{\mathbf{V}}}{\partial t} + \frac{\partial \mathbf{u}}{\partial t} + \bar{\mathbf{V}} \cdot \nabla \bar{\mathbf{V}} + \bar{\mathbf{V}} \cdot \nabla \mathbf{u} + \mathbf{u} \cdot \nabla \bar{\mathbf{V}} + \mathbf{u} \cdot \nabla \mathbf{u} = -\mathbf{e}_r \frac{\partial \bar{p}}{\partial r} - \nabla p' + \mathbf{e}_x P + \nabla^2 (\bar{\mathbf{V}} + \mathbf{u}). \quad (4)$$

From (2) it follows that $\bar{V}_z = 0$ everywhere. The cylinder average of (4) is

$$\begin{aligned} \frac{\partial \bar{\mathbf{V}}}{\partial t} + \mathbf{e}_r \left[\overline{\mathbf{u} \cdot \nabla w} - \frac{\bar{V}_\theta^2}{r} - \frac{v^2}{r} \right] + \mathbf{e}_\theta \left[\overline{\mathbf{u} \cdot \nabla v} + \frac{vw}{r} \right] + \mathbf{e}_x \overline{\mathbf{u} \cdot \nabla u} \\ = -\mathbf{e}_r \frac{\partial \bar{p}}{\partial r} + \mathbf{e}_x P + \mathbf{e}_\theta \left[\frac{1}{r} \frac{\partial}{\partial r} \left(r \frac{\partial \bar{V}_\theta}{\partial r} \right) - \frac{\bar{V}_\theta}{r^2} \right] + \frac{\mathbf{e}_x}{r} \frac{\partial}{\partial r} \left(r \frac{\partial \bar{V}_x}{\partial r} \right), \end{aligned} \quad (5)$$

and the difference (4) – (5) is

$$\begin{aligned} \frac{\partial \mathbf{u}}{\partial t} + \bar{\mathbf{V}} \cdot \nabla \mathbf{u} + \mathbf{u} \cdot \nabla \bar{\mathbf{V}} + \mathbf{u} \cdot \nabla \mathbf{u} - \mathbf{e}_r \left[\overline{\mathbf{u} \cdot \nabla w} - \frac{v^2}{r} \right] - \mathbf{e}_\theta \left[\overline{\mathbf{u} \cdot \nabla v} + \frac{vw}{r} \right] \\ - \mathbf{e}_x \overline{\mathbf{u} \cdot \nabla u} = -\nabla p' + \nabla^2 \mathbf{u}. \end{aligned} \quad (6)$$

Energy identities for the mean and fluctuating components are obtained by forming $\langle \bar{\mathbf{V}} \cdot (5) \rangle = 0$ and $\langle \mathbf{u} \cdot (6) \rangle = 0$, respectively. We also use $\bar{V}_r = 0$ and the following identity

$$\overline{\mathbf{u} \cdot \nabla f} = \overline{\nabla \cdot (\mathbf{u}f)} = \frac{1}{r} \frac{\partial}{\partial r} (r f \bar{w}),$$

which is valid when $\nabla \cdot \mathbf{u} = 0$. Thus,

$$\begin{aligned} \frac{1}{2} \frac{d}{dt} \langle |\bar{\mathbf{V}}|^2 \rangle + \left\langle \frac{\bar{u}\bar{w}\bar{V}_\theta}{r} + \frac{\bar{V}_\theta}{r} \frac{\partial}{\partial r} (r \bar{v}\bar{w}) + \frac{\bar{V}_x}{r} \frac{\partial}{\partial r} (r \bar{u}\bar{w}) \right\rangle \\ = P \langle \bar{V}_x \rangle - \left\langle \left| \frac{\partial \bar{V}_\theta}{\partial r} \right|^2 + \left| \frac{\partial \bar{V}_x}{\partial r} \right|^2 + \frac{\bar{V}_\theta^2}{r^2} \right\rangle, \end{aligned} \quad (7)$$

and

$$\frac{1}{2} \frac{d}{dt} \langle |\mathbf{u}|^2 \rangle - \left\langle \frac{\bar{u}\bar{w}\bar{V}_\theta}{r} - \bar{v}\bar{w} \frac{\partial \bar{V}_\theta}{\partial r} - \bar{u}\bar{w} \frac{\partial \bar{V}_x}{\partial r} \right\rangle + \Gamma = - \langle |\nabla \mathbf{u}|^2 \rangle. \quad (8)$$

Here

$$\Gamma = 2\overline{\phi(p'_w + \phi^2/2)}, \quad (9)$$

where p'_w is fluctuating pressure at the wall of the pipe. Summing (7) and (8) gives the total energy equation

$$\frac{1}{2} \frac{d}{dt} \langle |\bar{\mathbf{V}}|^2 + |\mathbf{u}|^2 \rangle = P \langle \bar{V}_x \rangle - \Gamma - \left\langle |\nabla \mathbf{u}|^2 + \left| \frac{\partial \bar{V}_\theta}{\partial r} \right|^2 + \left| \frac{\partial \bar{V}_x}{\partial r} \right|^2 + \frac{\bar{V}_\theta^2}{r^2} \right\rangle, \quad (10)$$

where it is noted that the second bracketed terms in (7) and (8) cancel.

3 Volume flux comparison between laminar and turbulent flows

First we consider laminar Hagen-Poiseuille flow, for which equation (1) has the solution

$$U_l(r) = 2 \langle U_l \rangle (1 - r^2) \quad (11)$$

for

$$P_l = 8 \langle U_l \rangle. \quad (12)$$

In order to evaluate the bulk flow rate for the turbulent flow cases, $\langle \bar{V}_x \rangle$, we specify two properties of statistical stationarity, assuming that a turbulent flow exists. The first is that all cylinder averages ($\bar{\quad}$) are time independent, and second we assume that velocity components have a zero mean value unless a non-zero mean value is forced externally. This latter property implies $\bar{V}_\theta = 0$. Under such conditions the x -component of equation (5) may be written as

$$\frac{d}{dr} \left[r \bar{u}\bar{w} - r \frac{d\bar{V}_x}{dr} - P \frac{r^2}{2} \right] = 0, \quad (13)$$

and the energy equation (8) becomes

$$\left\langle \overline{uw} \frac{d\bar{V}_x}{dr} \right\rangle + \Gamma = - \left\langle |\nabla \mathbf{u}|^2 \right\rangle. \quad (14)$$

We now seek an expression for P by taking the first integral of (13)

$$P \frac{r^2}{2} = r \overline{uw} - r \frac{d\bar{V}_x}{dr}. \quad (15)$$

Forming $\langle (15) \rangle$ gives

$$P = 4 \langle r \overline{uw} \rangle + 8 \langle \bar{V}_x \rangle. \quad (16)$$

A comparison between the volume flux in a pipe for a turbulent flow with control and the base laminar flow can now be made. For flows with the same driving pressure gradient ($P = P_l$), using (16) and (12) the difference between the bulk flow rates between fully developed laminar and turbulent flows is given by

$$\langle U_l - \bar{V}_x \rangle = \frac{1}{2} \langle r \overline{uw} \rangle. \quad (17)$$

Therefore a proof that zero-net volume flux blowing/suction control cannot produce a volume flux in excess of laminar flow requires

$$\langle r \overline{uw} \rangle \geq 0. \quad (18)$$

To test this we form $\langle \overline{uw} \cdot (15) \rangle = 0$ and using (14) obtain

$$\frac{1}{2} P \langle r \overline{uw} \rangle = \left\langle |\nabla \mathbf{u}|^2 \right\rangle + \left\langle [\overline{uw}]^2 \right\rangle - \Gamma. \quad (19)$$

Here $P > 0$ by definition, and therefore, the controlled flow can produce a volume flux in excess of laminar flow if, and only if,

$$\Gamma > \left\langle |\nabla \mathbf{u}|^2 \right\rangle + \left\langle [\overline{uw}]^2 \right\rangle. \quad (20)$$

The same criterion holds for producing sub-laminar drag as will be discussed in the following section.

3.1 Quantitative comparisons

For pipe flow without flow control (where $\Gamma = 0$), equations (17) and (19) show that the flow rate in laminar flow is always higher than in turbulent flow at the same pressure gradient. This was first proven by Thomas [3], and while generally well known, we are not aware of any formulas in the literature that quantifies these volume flux differences. Quantitative differences between the bulk flow rates can be obtained using functional forms for the mean velocity profiles (laminar and turbulent). Following MJM, using a law of the wall-wake mean velocity formulation ([4]) it can be shown that, to a good approximation,

$$\langle \bar{V}_x \rangle = Re_\tau \left(\frac{\bar{V}_1}{U_\tau} - \frac{3}{2\kappa} \right) \quad (21)$$

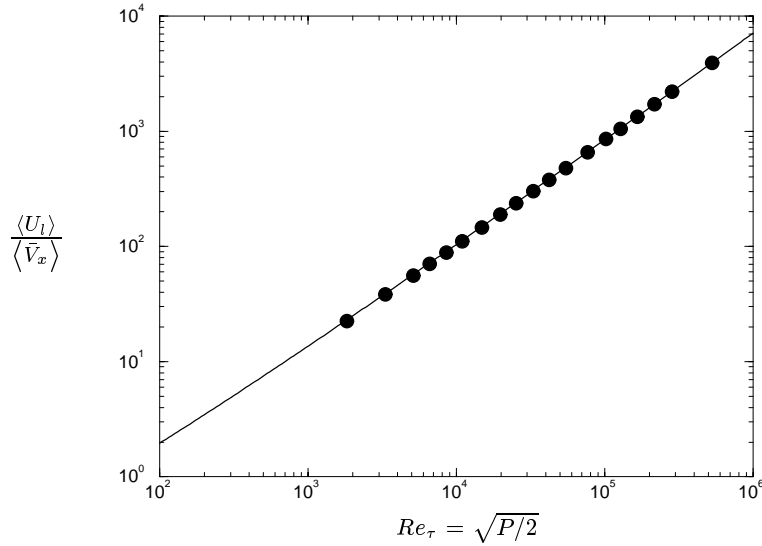


Fig. 1. Ratio of bulk velocities for laminar and turbulent pipe flows as a function of Re_τ . The filled circles are from pipe experiments [5].

with

$$\frac{\bar{V}_1}{U_\tau} = \frac{1}{\kappa} \ln(Re_\tau) + 5.16 \quad (22)$$

where \bar{V}_1 and U_τ are the nondimensional center-line and skin friction velocities respectively. (Here $Re_\tau = a\hat{U}_\tau/\nu = U_\tau$.) For laminar flow

$$\langle U_l \rangle = \frac{Re_\tau^2}{4}. \quad (23)$$

Figure 1 shows the resulting comparison between the bulk velocities for laminar and turbulent flows for varying levels of Re_τ compared to the experimental data of McKeon *et al.* [5] obtained in the Princeton superpipe. It is noted that for a typical practical Reynolds number of $Re_\tau = 10^5$ the ratio $\langle U_l \rangle / \langle \bar{V}_x \rangle$ is seen to be over 1000.

4 Drag comparisons for pipe flow

For a fully developed pipe flow with statistical stationarity, the net skin friction drag is simply obtained from a balance with the pressure gradient forces. That is,

$$\hat{\tau}_0(4\pi aL) = \rho\hat{P}(2\pi a^2L)$$

where $\hat{\tau}_0$ and \hat{P} are dimensional average wall-shear stress and driving pressure gradient respectively. From this it follows that the bulk skin friction coefficient

$C_f = 2\hat{\tau}_0/(\rho\hat{U}_B^2)$, where \hat{U}_B is dimensional bulk velocity, is related to P by

$$C_f = \frac{P}{Re_B^2}. \quad (24)$$

Using (16), (12) and (24) for a given Reynolds number $\langle U_l \rangle = \langle \bar{V}_x \rangle = Re_B$, we obtain

$$C_f - C_{f_l} = \frac{4}{Re_B^2} \langle r\overline{uw} \rangle. \quad (25)$$

Equation (25) is equivalent to the result obtained by Fukagata *et al.* [6] where they showed that drag reduction is dependent on the weighted integral of Reynolds shear stress.

As expected, the criteria for achieving sub-laminar drag, with control for a fixed volume flux, is equivalent to exceeding the volume flux of laminar flow for a fixed pressure gradient. Both depend on $\langle r\overline{uw} \rangle$. Therefore, for controlled flows to produce sustained sub-laminar skin friction levels requires

$$\Gamma > \langle |\nabla \mathbf{u}|^2 \rangle + \langle [\overline{uw}]^2 \rangle.$$

5 Concluding remarks

The result in figure 1 indicates that at very high Re_τ the flow rates in pipes would be phenomenally (and likely aphysically) high for a laminar flow compared to the turbulent case. This would indicate that while sub-laminar conditions require the criterion in equation (20) to hold, other factors likely related to stability need to be considered. Also, the similarity between equation (20) in this paper, and the corresponding expression derived by MJM for a plane channel, suggests that MJM's conclusions about sub-laminar drag control strategies in plane channels, are equally valid for pipe flows.

Acknowledgments. This work was in part supported by the National Science Foundation (IM with CTS-0324898, DDJ with CTS-0302837 and KM with CTS-0133837), and the David and Lucile Packard Foundation.

References

1. I. Marusic, D.D. Joseph, and K. Mahesh. Laminar and turbulent comparisons for channel flow and flow control. *J. Fluid Mech.*, 570:467–477, 2007.
2. T. Min, S.M. Kang, J. L. Speyer, and J. Kim. Sustained sub-laminar drag in a fully developed channel flow. *J. Fluid Mech.*, 558:309–318, 2006.
3. T. Y. Thomas. Qualitative analysis of the flow of fluids in pipes. *Amer. J. Math*, 64:754–767, 1942.
4. A. E. Perry, I. Marusic, and M. B. Jones. On the streamwise evolution of turbulent boundary layers in arbitrary pressure gradients. *J. Fluid Mech.*, 461:61–91, 2002.
5. B.J. McKeon, J.D. Li, W. Jiang, J.F. Morrison, and A.J. Smits. Further observations on the mean velocity in fully-developed pipe flow. *J. Fluid Mech.*, 501:135–147, 2004.
6. K. Fukagata, K. Iwamoto, and N. Kasagi. Contribution of Reynolds stress distribution to the skin friction in wall-bounded flows. *Phys. Fluids*, 14(11):L73–L76, 2002.